International Journal of Biological Macromolecules 149 (2020) 127–139

Contents lists available at ScienceDirect

International Journal of Biological Macromolecules

journal homepage: http://www.elsevier.com/locate/ijbiomac

Impregnation of magnetic - *Momordica charantia* leaf powder into chitosan for the removal of U(VI) from aqueous and polluted wastewater

Gutha Yuvaraja [a,b], Minhua Su [a,b], Di-Yun Chen [a,b,*], Yixiong Pang [a,b], Ling-Jun Kong [a,b,*], Munagapati Venkata Subbaiah [c], Jet-Chau Wen [c,d], Guda Mallikarjuna Reddy [e]

[a] Guangdong Provincial Key Laboratory for Radionuclides Pollution Control and Resources, School of Environmental Science and Engineering, Guangzhou University, Guangzhou, 510006, China
[b] School of Civil Engineering, Guangzhou University, Guangzhou 510006, PR China
[c] Research Centre for Soil & Water Resources and Natural Disaster Prevention (SWAN), National Yunlin University of Science & Technology, 123, Section 3, University Road, Douliou, Yunlin 640, Taiwan, ROC
[d] Department and Graduate School of Safety and Environment Engineering, National Yunlin University of Science & Technology, 123, Section 3, University Road, Douliou, Yunlin 640, Taiwan, ROC
[e] Ural Federal University, Chemical Engineering Institute, Yekaterinburg 620002, Russian Federation

ARTICLE INFO

Article history:
Received 29 August 2019
Received in revised form 13 January 2020
Accepted 20 January 2020
Available online 21 January 2020

Keywords:
U(VI) removal
Kinetics
Isotherms

ABSTRACT

Uranium (U(VI)) is radioactive and the primary raw material in the production of nuclear energy. Hence the research associated with uranium removal gained a lot of importance because to reduce the threat of uranium contamination to ecology and its environment surroundings. Thus, economically as well as environmentally friendly sorbents with a good sorption capacity have to be acquired for the removal of U(VI) pollutants from the aqueous and polluted sea samples. In this study magnetic- *Momordica charantia* leaf powder impregnated into chitosan (m-MCLPICS) was prepared through the impregnation method. After preparation the adsorbent undergone through various characterizations such as BET, XRD, FTIR, SEM with elemental mapping, and VSM analysis. The specific surface area (93.12 m^2/g), pore size (0.212 cm^3/g) and pore volume (15.35 nm) of m-MCLPICS was obtained from the BET analysis. A pH value of 5 and 0.5 g of adsorbent dose were selected as an optimum values for U(VI) removal. Kinetic data follows the pseudo-second-order model, and the equilibrium data fitted well with the Langmuir isotherm model. ΔG° (−1.6999, −2.4994, −3.5476 and −4.5147 kJ/mol), ΔH^0 (25.1 kJ/mol) and ΔS^0 (0.089 kJ/mol K) indicates that the U(VI) sorption process is feasible, spontaneous and endothermic.

1. Introduction

Water is a basic requirement for the entire organism in this world. Most of the industries are being set up near water bodies. As a result water pollution is a major environmental issue at the moment. The main source of nuclear energy is uranium (U(VI)) and it has been introduced into nature through nuclear operations, such as nuclear power stations, nuclear fuel production, nuclear testing, and nuclear mishaps [1]. Uranium is mainly found in two oxidation stages in the earth's crust, i.e. U(IV) and U(VI) [2]. U(VI) seems to be extremely water-soluble and can quickly develop complexes with carbonate in groundwater and U(IV) is precipitated into UO_2(s) [3]. U(VI) toxicology can cause significant damage in humans such as hepatitis, corrosion of the skin, damage to the histopathological system, irreversible renal injuries, urinary tract disorders, DNA damage, and some types of cancer [4,5]. Therefore, the removal of U(VI) from aqueous and real polluted solutions has been extensively investigated using a variety of adsorbents.

Up to now, a variety of methods, such as complexation [6], reduction [7], solid phase extraction [8], ion-exchange [9], solvent extraction [10], membrane processes [11], and adsorption [12] have been used to remove uranium from the contaminated water sources. Among these methods, adsorption is considered to be a suitable and promising method to remove toxic contaminants from wastewater owning to its operation, high efficiency and cost-effectiveness [13]. Adsorption can be considered as a most popular method for the removal of organic and inorganic pollutants from aqueous solutions [14–34]. Adsorbent prepared from natural polymer and biopolymer is attractive because of their minimal effort and simple access. Hence chitosan can be considered as a perfect adsorbent due to bottomless free amino and hydroxyl bunches on its spine. Chitosan and its derivate forms has potential applications in the fields of biotechnology, biomedicine and cosmetics because of their unique properties such as hydrophilicity, biocompatibility, biodegradability and anti-bacterial property. Various adsorbents such as graphene oxide nanosheets [35], activated carbon [36], Graphene Oxide/Chitosan Aerogel [37], Crystalline Tin Oxide Nanoparticles [38], Calcined and Acid Activated Kaolin [39], Magnetic Chitosan Resins [40], natural and modified diatomite [41], CTPP beads [42], ion-imprinted magnetic chitosan resins [43], Aloe vera wastes

* Corresponding author.
E-mail addresses: cdy@gzhu.edu.cn (D.-Y. Chen), kongl_ju@163.com (L.-J. Kong).

https://doi.org/10.1016/j.ijbiomac.2020.01.200
0141-8130/

[44], and chitin/chitosan-bearing materials [45] was utilized for the removal of U(VI) from aqueous media. Adsorbent preparation is simple and inexpensive in impregnation method. At the same time the combination of chitosan with magnetic leaf powder gained a lot of importance due to their easy preparation and good biocompatibility. In this way first we prepared magnetic-leaf powder. After that we impregnated the magnetic leaf powder into the chitosan polymer to prepare a novel sorbent material with high sorption capacity. We got the fruitful results on pollutant wastewater.

Here we report the preparation, characterization and application of m-MCLPICS as adsorbent for removing U(VI) from aqueous and real polluted water samples. U(VI) removal was achieved with appropriate pH (pH 5 for aqueous and 1.2, 3.3 and 8.1 with real polluted samples) and dose values (dose 0.5 g). Pseudo-first-order, and pseudo- second-order, models were applied to investigate the kinetics mechanism of m-MCLPICS towards U(VI) ions. Equilibrium experiments (Langmuir, Freundlich, and D-R isotherm models) were performed with temperature dependence to evaluate sorption efficiency toward uranium ions. Thermodynamic study was also performed to evaluate sorption efficiency of U(VI) onto m-MCLPICS.

2. Materials and methods

2.1. Materials

Chitosan obtained from Sigma–Aldrich with deacetylation degree of 75–85%. Glacial acetic acid, sodium hydroxide sodium (NaOH, S.L., Spain), sulfuric acid (H_2SO_4, Sigma–Aldrich, Germany), $FeCl_3.2H_2O$, $FeCl_3.6H_2O$ (Sigma–Aldrich, Germany) and U(VI) ($UO_2(NO_3)_2.6H_2O$ 98%, Sigma–Aldrich, Germany) were used without further purification. Uranium stock solution was prepared by dissolving uranyl nitrate hexahydrate ($UO_2(NO_3)_2.6H_2O$) in double distilled water.

2.2. Preparation of m-MCLPICS

m-MCLPICS was prepared by impregnation method. 2 g of $FeCl_3.2H_2O$ and 2 g of $FeCl_3 \cdot 6H_2O$ were dissolved 50 mL of distilled water and the solution was stirring continuously to make the clear solution. *Momordica charantia* leaves were took from the Guangzhou university surroundings. The leaves were washed, dried and made into fine powder. 0.2 g of NaOH was dissolved in 25 mL of water and it was added to the solution. The solution was turned into black color immediately. It was vigorously stirred for 30 min. Then the magnetic leaves powder was washed thoroughly with distilled water and dried in an oven at 50 °C for 7 h.

Two grams of chitosan powder was dissolved in 100 mL of glacial acetic acid solution. The solution was kept at constant stirring for 3 h to make the clear chitosan solution. To the chitosan solution the magnetic leaf powder was added and stirred for 4 h. With the help of micro-pipette the solution was dropped into the beaker containing 0.1 N NaOH solution. After falling into the NaOH solution the material was formed into solid material. Then the material was separated from the NaOH solution and washed thoroughly with distilled water. Finally it was dried at 50 C temperature for 12 h and it was named as m-MCLPICS for further representation.

2.3. Batch sorption experiments

Removal of U(VI) onto m-MCLPICS was carried out in 50.0 mL polyethylene tubes. pH of the solution was adjusted by adding negligible volume of 0.1N NaOH or HCl. pH experiments were done by varying the pH from 2 to 10 with 40 mg/L concentration at room temperatures. Adsorbent dose experiments varied from 0.1 to 0.7 g with the 40 mg/L initial U(VI) concentration. The agitation experiments confirmed that 200 min shaking time was enough to achieve sorption equilibrium. Kinetic studies were performed at different time intervals (0–420 min). The initial U(VI) concentration was 20–80 mg/L. Isotherm studies were performed at different temperatures (298, 308, 318 and 323 K). These samples were placed in a shaker and stirred up at 90 min. After certain time the samples were taken out from the shaker, filtered and the U(VI) concentration was analyzed . Every assessment was repeated two times and its average value has been given. The adsorbed quantity of U(VI) at equilibrium was achieved by the following equation:

$$q_e = \frac{(C_i - C_e)V}{M} \quad (1)$$

where, q_e (mg/g) was the adsorption capacity at equilibrium, C_i and C_e were initial and equilibrium level of U(VI) (mg/L), M (g) was the adsorbent dose, and V (L) was solution volume.

2.4. Characterization of adsorbent

From BET and D-R equations the specific surface area and pore volume of the adsorbent was calculated. In order to study the overall pore volumes, which correspond to the sum of micropores and mesopores, N_2 adsorbed at relative pressure (P/Po = 0.98) was used. XRD with Cu Kα radiation (λ = 1.5418 Å) operated at 2000 W power and a scanning rate of 10°/min in the 2θ range from 10 to 90. To evaluate the functional groups, the adsorbent was characterized by FTIR studies with Nicolet IS10, Thermo Scientific, USA. 10 mg sample was blended with 100 mg of KBr and ground into a pellet for IR spectral studies. A plain KBr pellet was taken to measure the background absorbance. Surface morphology and elemental compositions of samples were measured using a JEOL JSM-7001F Japan, scanning electron microscope (SEM). Magnetic nature of the adsorbent was performed with a vibrating sample magnetometer (VSM, LakeShore-7404).

2.5. Reusability test

0.5 grams of m-MCLPICS was applied to a plastic centrifuge tube that contained U(VI) solution (30 mL, 20 mg/L), and the reusability was measured at the desired pH. The suspensions were filtered after six hours of shaking, and the metal ion content was measured in the filtrate in order to achieve the adsorption efficiency of the sorbent. In order to remove non-adsorbed metal ions, the metal loaded m-MCLPICS was collected and washed three times carefully with distilled water. After that the m-MCLPICS was agitated for 4 h with 10 mL with 0.01 mol/L of EDTA solution. In the aqueous solution, the final concentration of U(VI) was estimated by AES. The U(VI) desorption ratio was calculated from the m-MCLPICS. The adsorption-desorption process was performed seven times with the same affinity adsorbent in order to test the reusability of the sorbent. By using the following equation the performance of the U(VI) desorption was assessed.

$$\text{Desorption efficiency} = \frac{\textit{Amount of U(VI) desorbed}}{\textit{Amount of U(VI) adsorbed}} \times 100 \quad (2)$$

3. Results and discussion

3.1. BET analysis

BJH adsorption/desorption method was applied to find out the surface area, pore volume and diameter of MCLP, m-MCLP and m-MCLPICS. The specific surface areas of MCLP, m-MCLP and m-MCLPICS were 46.09, 69.06 and 93.12 m^2/g. The pore size of MCLP, m-MCLP and m-MCLPICS were 0.151, 0.183 and 0.212 cm^3/g. Whereas the pore volume of MCLP, m-MCLP and m-MCLPICS were 8.41, 11.09 and 15.35 nm in size. Surface area of the material was increased with modification. In addition to this the pore volume and diameter will also increase. The increase in surface area pore, volume and diameter reveals

the successful functionalization was done on the surface of the materials.

3.2. XRD analysis

Crystal/amorphous nature of the material has been identified from the XRD analysis. Fig. 1 (from 1A–D) represents the XRD analysis of MCLP, m-MCLP, m-MCLPICS and U(VI) loaded m-MCLPICS. In MCLP spectrum we found two broad and strong peaks. In m-MCLP spectrum the intensity of the two amorphous peaks (belongs to the MCLP) were decreased and the 4 well resolved new peaks were identified. The new peaks in m-MCLP represents the nature of the material with crystallinity. Whereas in m-MCLPICS the peaks were present and it represents the impregnation was done properly without changing the nature of the material. After U(VI) sorption, the intensity and the crystallinity was decreased. Hence we may expect that m-MCLPICS has undergone U(VI) sorption successfully.

3.3. FTIR analysis

FTIR spectra of the MCLP, m-MCLP, m-MCLPICS and U(VI) loaded m-MCLPICS were shown in Fig. 2A-D. Broad band appears 3446 cm^{-1}, reveals the stretching vibration of —OH and —NH groups. The two peaks at 2933 cm^{-1} and 1797 cm^{-1} represents the aliphatic C—H stretching vibration in the —CH_2 group and C═O respectively. The peak at 1642 cm^{-1} shows the presence of free amine. Whereas the peak at 1612 cm^{-1} represents the bending vibrations of —NH group. The band at 1065 cm^{-1} is attributed to the combined effects of C—N stretching vibration of primary amines and the C—O stretching vibration from the primary alcohol. The two peaks at 896 and 798 cm^{-1} refers the N—H deformational vibrations in the secondary amine.

In m-MCLP the peak at 3433 cm^{-1} attributed to the overlapped stretching vibrations of -OH and NH functional groups present in the chitosan. Peak at 2927 cm^{-1} corresponded to stretching vibrations of O—H/N—H and C—H. 1650 cm^{-1} correspond to the bending N—H in amide groups. The band at 1041 cm^{-1} is assigned to the —CO stretching vibration of —C—OH. The band at 570 cm^{-1} is attributed to Fe—O stretching vibration.

m-MCLPICS has the broad and strong band at 3452 cm^{-1} is assigned to the amino (—NH_2) and hydroxyl (—OH) stretching vibrations. The sharp peak at 2926 cm^{-1} is due to C—H anti symmetric stretching vibration and peaks at 1648 and 1599 cm^{-1} (C═O stretching vibration of amide and the bending vibration of —NH_2 groups), 1072 cm^{-1} (skeletal vibration involving the C—O stretching). A band at 1060 cm^{-1} is attributed to the C—O—C of carbohydrate structure. A new peak appeared at 580 cm^{-1}, corresponds to the Fe-O group, indicating that m-MCLP was successfully impregnated into the chitosan.

The shift in the peak (U(VI) loaded m-MCLPICS) at 3452 to 3422 cm −1 (—OH stretching vibration). The peak at 2920 cm^{-1} was attributed to —CH stretching vibration in —CH and —CH_2. The peaks at 1655 and 1599 cm^{-1} are related to the C═O stretching vibration of amide and the bending vibration of —NH_2 groups. These peaks shifting and the change in the intensity of the characteristic peaks may have been because the amino and hydroxyl groups are the major functional groups involved in U(VI) removal.

3.4. SEM with elemental mapping

SEM analysis of MCLP, m-MCLP, m-MCLPICS and U(VI) loaded m-MCLPICS were shown in Fig. 3A-D. MCLP (Fig. 3A) having smooth surface. An irregular rough surface was found in m-MCLP (Fig. 3B). As shown in Fig. 3C, before sorption process the sorbent has the smooth

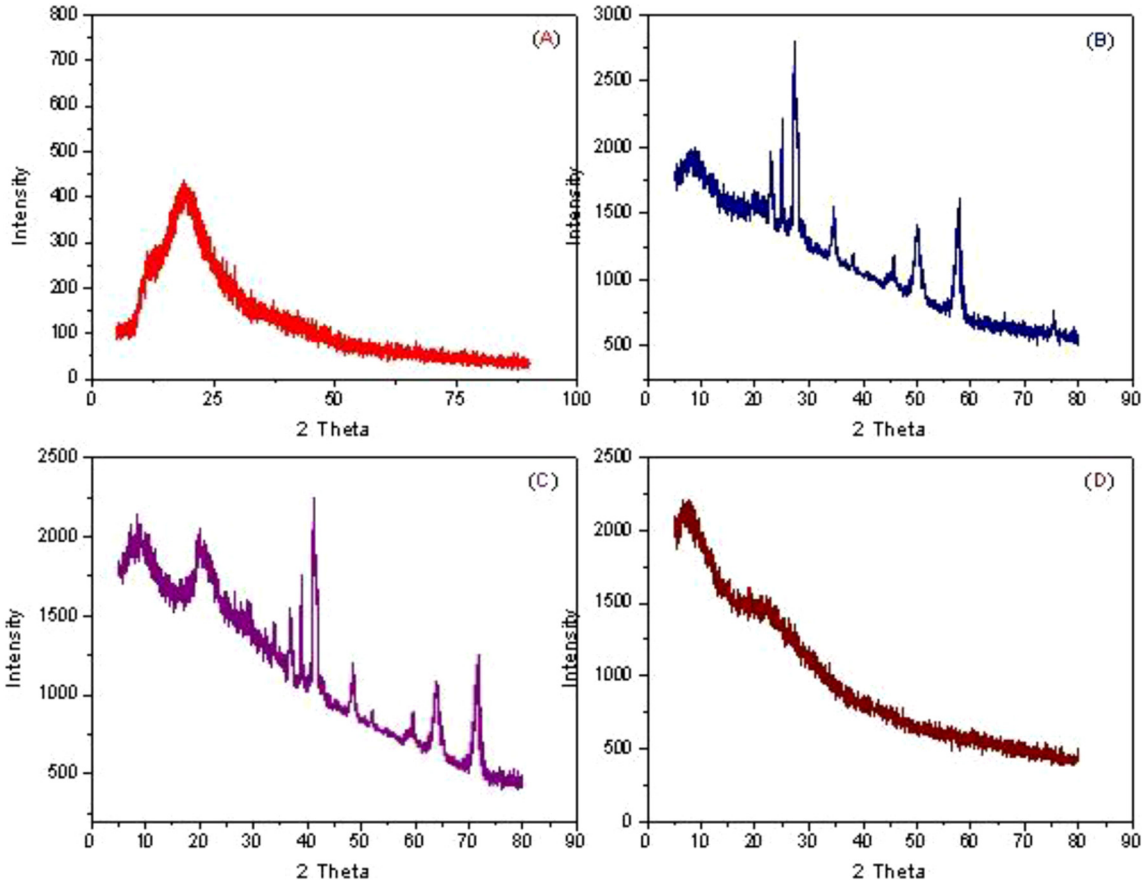

Fig. 1. XRD analysis of (A) MCLP; (B) m-MCLP; (C) m-MCLPICS; and (D) U(VI) loaded m-MCLPICS.

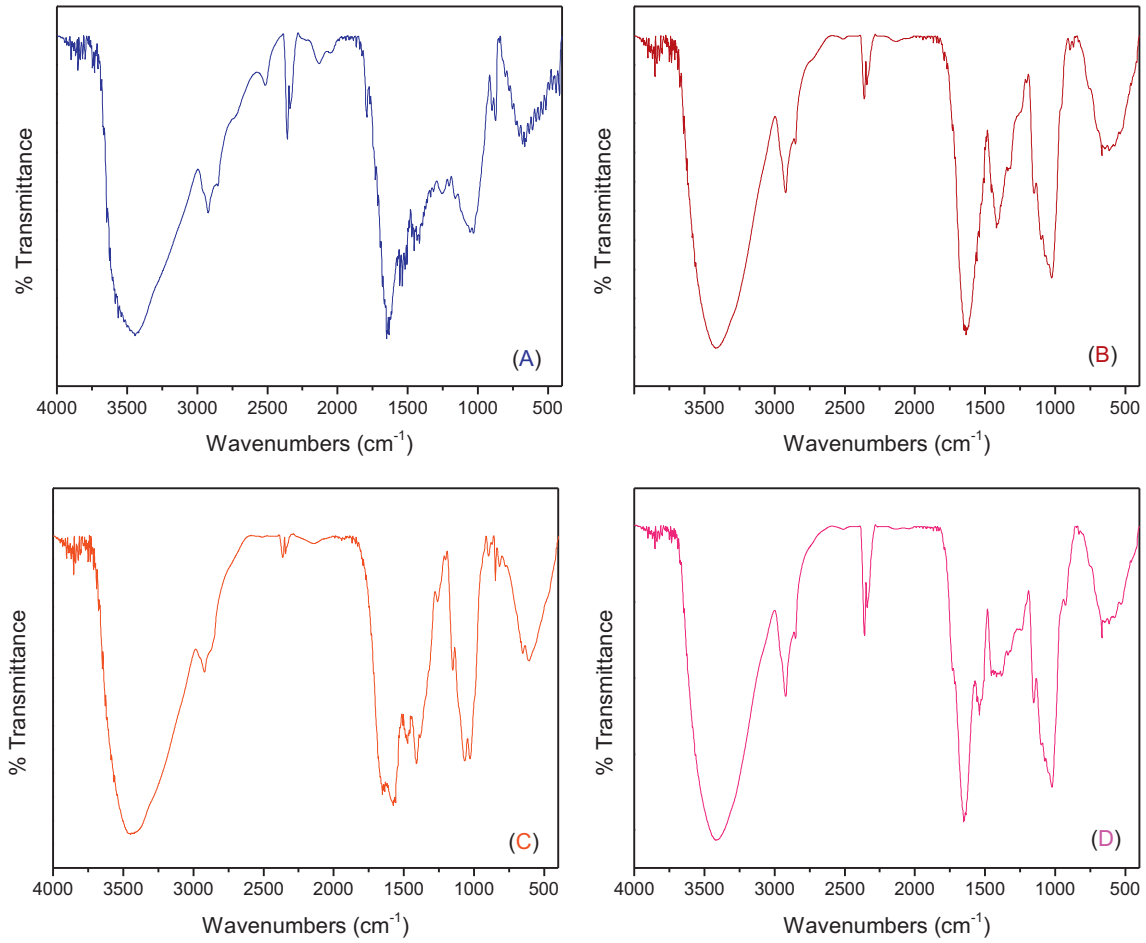

Fig. 2. FTIR spectral analysis of (A) MCLP; (B) m-MCLP; (C) m-MCLPICS; and (D) U(VI) loaded m-MCLPICS.

surface with plates and nearly regular surface. After sorption all the U (VI) ions were deposited on the adsorbent surface (Fig. 3D), a granular substance adhering to the surface of the entity was observed. After U (VI) sorption (Fig. 3D) the surface of the m-MCLPICS was totally changed. Elemental mapping of MCLP, m-MCLP, m-MCLPICS and U(VI) loaded m-MCLPICS were shown in Fig. 4. Pure MC exhibited the presence of C, N, O, and S elements on it. And m-MCLP having the C, N, O, S, and Fe groups in it. In m- MCLP a new Fe elemental group was observed. This represents that the magnetization was successfully done. Before sorption m-MCLPICS having the C, N, O, S, and Fe groups in it. After U(VI) sorption U was also found along with the C, N, O, and S groups. Hence U(VI) sorption was done successfully with m-MCLPICS.

3.5. Magnetic analysis

Magnetic property of m-MCLP, m-MCLPICS and U(VI) loaded m-MCLPICS was done with VSM analysis and the results were kept in Fig. 5. m-MCLP is having the highest 36.64 emu/g value. And m-MCLPICS (30.12.34 emu/g) possess the lower value than the magnetic algae powder. Loss of magnetization in m-MCLPICS was due to the impregnation. U(VI) loaded m-MCLPICS has the less magnetization value compared with the m-MCLPICS (25.24 emu/g). This is because the U(VI) ions have been completely interacted with surface active sites.

3.6. Effect of pH

In the adsorption process, pH is a critical control parameter. pH has an influence on the surface of the adsorbent as well as the speciation of the adsorbate and its mechanism was shown in Fig. 6A-C. The initial U(VI) concentration was taken as 40 mg/L for pH experiments. Fig. 6C represents the effect of pH ranging from 1 to 10 for the removal of U(VI) onto m-MCLPICS. At lower pH the U (VI) removal percentage is low. UO_2^{2+} ions are the dominate species in the system when pH was below 4.0. And most of the adsorbent active sites are protonated, leading to the relatively low amounts of U (VI) removal below pH 4.0. H^+ ion concentration is very high (at low pH levels) and may leads to form another kind of interaction (ion exchange mechanism)) in acidic conditions. The removal percentage of U(VI) onto m-MCLPICS increases with the increasing pH from 2 to 5. The involvement of functional groups in the mechanism of U(VI) sorption system by m-MCLPICS was elucidated well with ion exchange, electrostatic attraction, and complexation/coordination. Nitrogen and oxygen are having lone pair of electrons. They can form the complex with the metal U(VI) through an electron pair sharing. The main reason for this one is surface complexation. Another reason is electrostatic attraction was occurred between the negative charge m-MCLPICS and positive charge UO_2^{2+}. During the mechanism the carboxyl group was deprotonated and the m-MCLPICS surface became negative. Hence automatically the negative surface can attract the positive U(VI) ions through electrostatic attraction forces. During the electrostatic attraction the U(VI) removal percentage was less. Whereas the removal percentage of U(VI) onto m-MCLPICS decreases when pH > 5. This was affected by the deprotonation mechanism and the potent electrostatic repulsion occurred between the negatively charged m-MCLPICS and negatively charged hydroxyl uranyl. Thus all the U(VI) adsorption studies were carried out at pH 5.0.

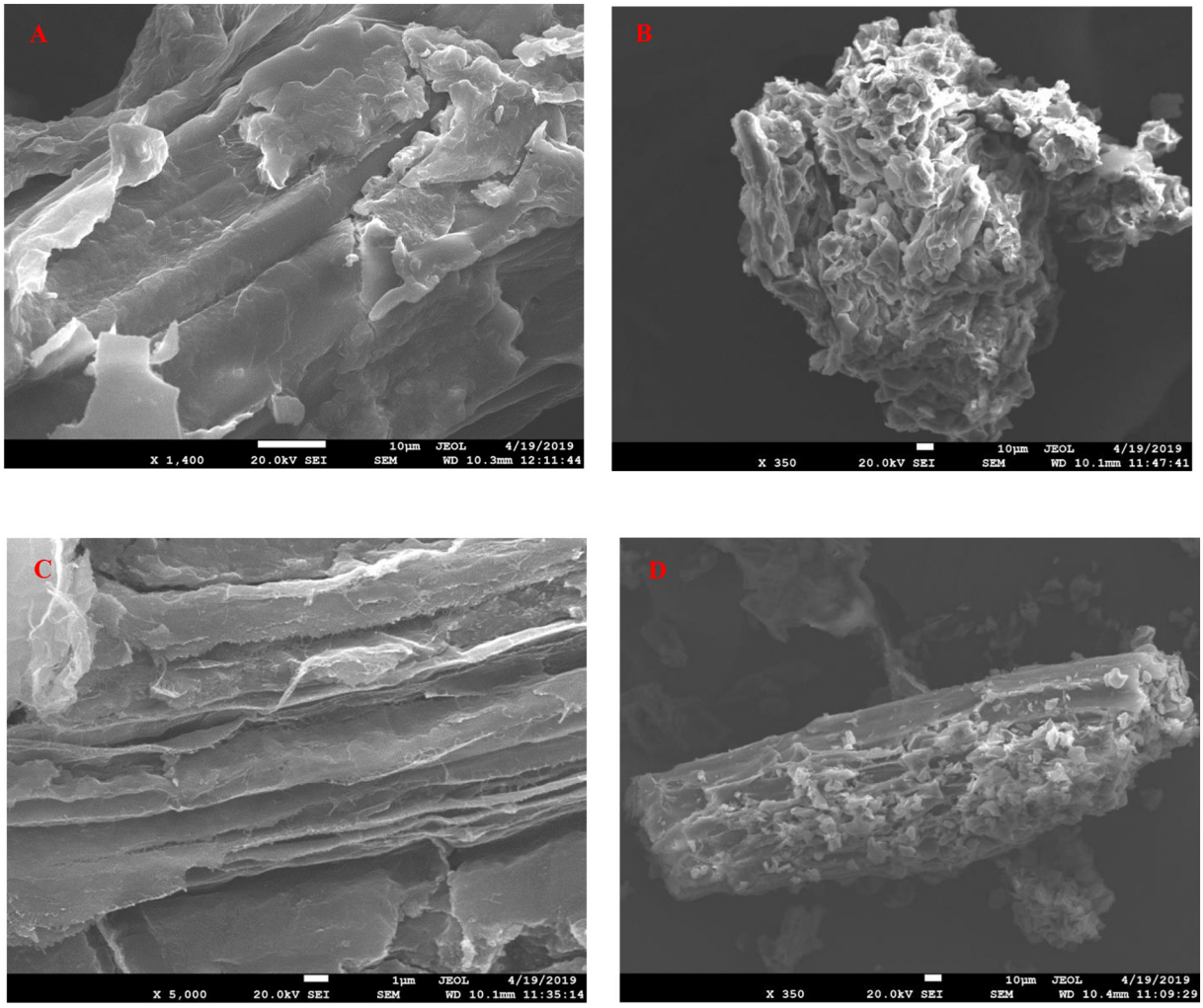

Fig. 3. Morphological analysis (SEM) of (A) MCLP, (B) m-MCLP, (C) m-MCLPICS, and (D) U(VI) loaded m-MCLPICS.

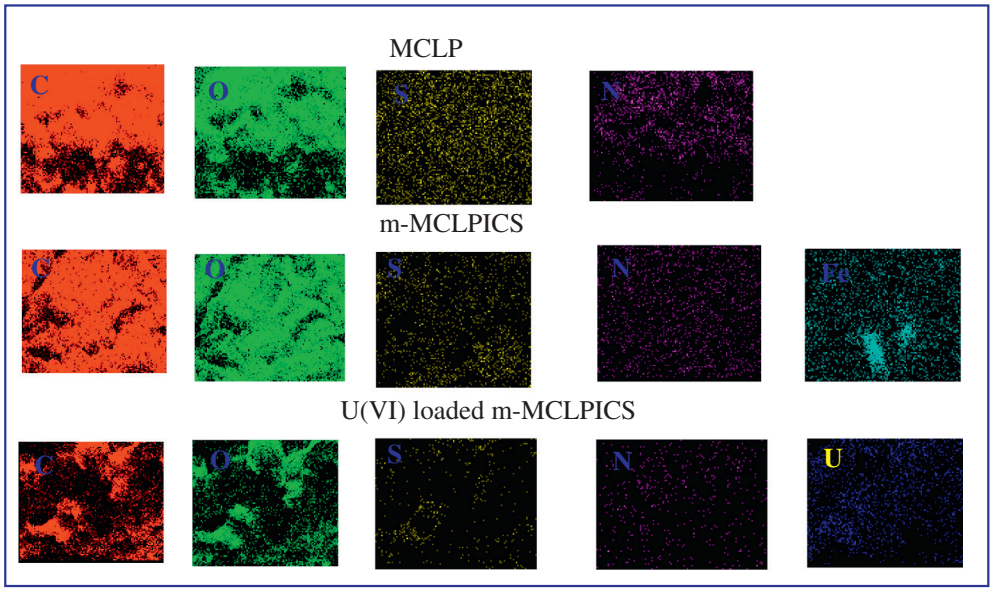

Fig. 4. Elemental mapping of (A) MCLP; (B) m-MCLPICS; and (C) U(VI) loaded m-MCLPICS.

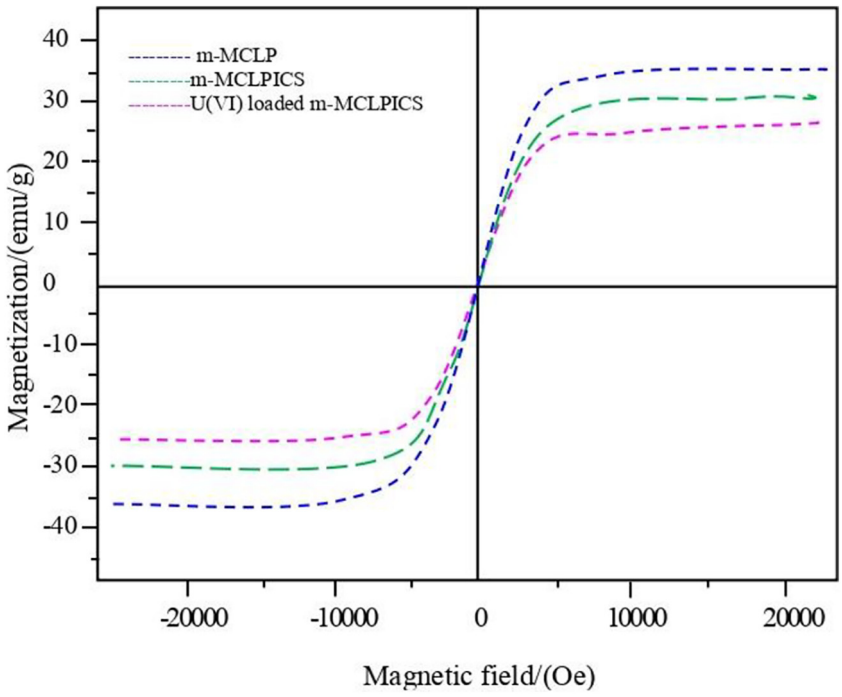

Fig. 5. Magnetization measurement of m-MCLP, m-MCLPICS and U(VI) loaded m-MCLPICS.

3.7. Effect of adsorbent dose

Dose is the crucial parameter in adsorption system. Removal of U(VI) onto m-MCLPICS was done with different dose values to attain an adequate relationship among the sorbent dosage as well as the sorption efficiency. In this study adsorbent was varied between 0.1 and 0.7 g by maintain all other parameters constant (pH 5, initial U(VI) concentration 40 mg/L, equilibrium time 120 min). As shown in Fig. 6D, with an increase in the sorbent dosage, U(VI) removal efficiency increases. It can be attributed that the adsorbing material has more active sites and more functional groups accessible on the surface. The removal efficiency almost reached a maximum when the dosage was increased to 0.5 g/L and remained stable with further increases in a sorbent dose. The sorption capacity for the m-MCLPICS is almost unchanged as the dosage increases further. Therefore, the above results show that the 0.5 g of sorbent dose can be considered an ideal value for the removal of U(VI) from water.

3.8. Effect of contact time

To know the removal efficiency of the adsorbent, experiments were explored with the different contact time (0–420 min) at pH 5.0 with the initial U(VI) concentration of 20–80 mg/g. Rate-controlling steps (mass transport or chemical reaction) can be obtained from the contact time studies. Contact time studies were shown in Fig 6E. It is evident that at the first 30 min the adsorption rate increases quickly and appears to be stable. That is because more active sites are available at the starting of the adsorption process and, after a while, the adsorbent sites are progressively occupied by an adsorbent which really accelerates the adsorption process. The equilibrium was achieved within 90 min. The amount of adsorbed U(VI) did not show any changes after equilibrium period. On the basis of above results, 90 min of contact time have been considered as an optimum time for further U(VI) sorption experiments.

3.9. Kinetic experiments

Pseudo-first-order [46] (Eq. (2)), and pseudo-second-order [47] (Eq. (3)) were utilized to investigate the kinetic data of the reaction.

$$q_t = q_{e1}(1- \exp(-k_1 t)) \tag{3}$$

$$q_t = \frac{q_{e2}^2 k_2 t}{1 + q_{e2} k_2 t} \tag{4}$$

where qe (mg/g) and qt (mg/g) are the amounts of U(VI) sorbed at equilibrium and at time t. K_1, and K_2 represents the rate constants for first-order, and second-order kinetic process. The kinetic parameters (K_1, K_2 and R^2) obtained by non-linear regression method are tabulated in Table 1. The non-linear sorption kinetic curves for U(VI) are shown in Fig. 6F-I. The relatively low values of R^2 indicate that the pseudo-first-order kinetic model is not fit for analyzing the adsorption process. Low values of R^2 demonstrate that the kinetic model of the pseudo-first order is unsuitable for adsorptive analysis. Pseudo-second-order R^2 values are higher than pseudo-first-order kinetic values. This will also suggests that the pseudo-second-order is the best fit to the experimental data and the chemisorption can be considered as the dominant mechanism in this study. Hence rate-controlling step (chemisorption) might involve in the valence forces through sharing of electrons between adsorbent and U(VI) ions [48].

3.10. Isotherms

Adsorption isotherm experiments were carried out to know the nature of the adsorption process and its mechanism. Langmuir [49], Freundlich [50] and D-R isotherm [51] models were applied (Fig. 6J) to know the equilibrium data. The three isotherm models were represented by the following equations.

$$q_e = \frac{q_m K_L C_e}{1 + K_L C_e} \tag{5}$$

$$q_e = K_f C_e^{1/n} \tag{6}$$

$$q_e = q_m \exp(-K\varepsilon^2) \quad (7)$$

$$\text{where } \varepsilon = RT \ln\left(1 + \frac{1}{C_e}\right) \quad (8)$$

where q_m (mg/g) is the amount of U(VI) adsorbed onto a unit mass of adsorbent, q_m (mg/g) is the maximum sorption capacity of the adsorbent, K_L and K_f (L/mg) are constants off Langmuir and Freundlich, C_e (mg/L) is the equilibrium concentration of adsorbate, n is the Freundlich exponent, ε is the Polanyi potential, R is the ideal gas constant (8.314 J/mol K) and T is the absolute temperature in Kelvin. Langmuir Model

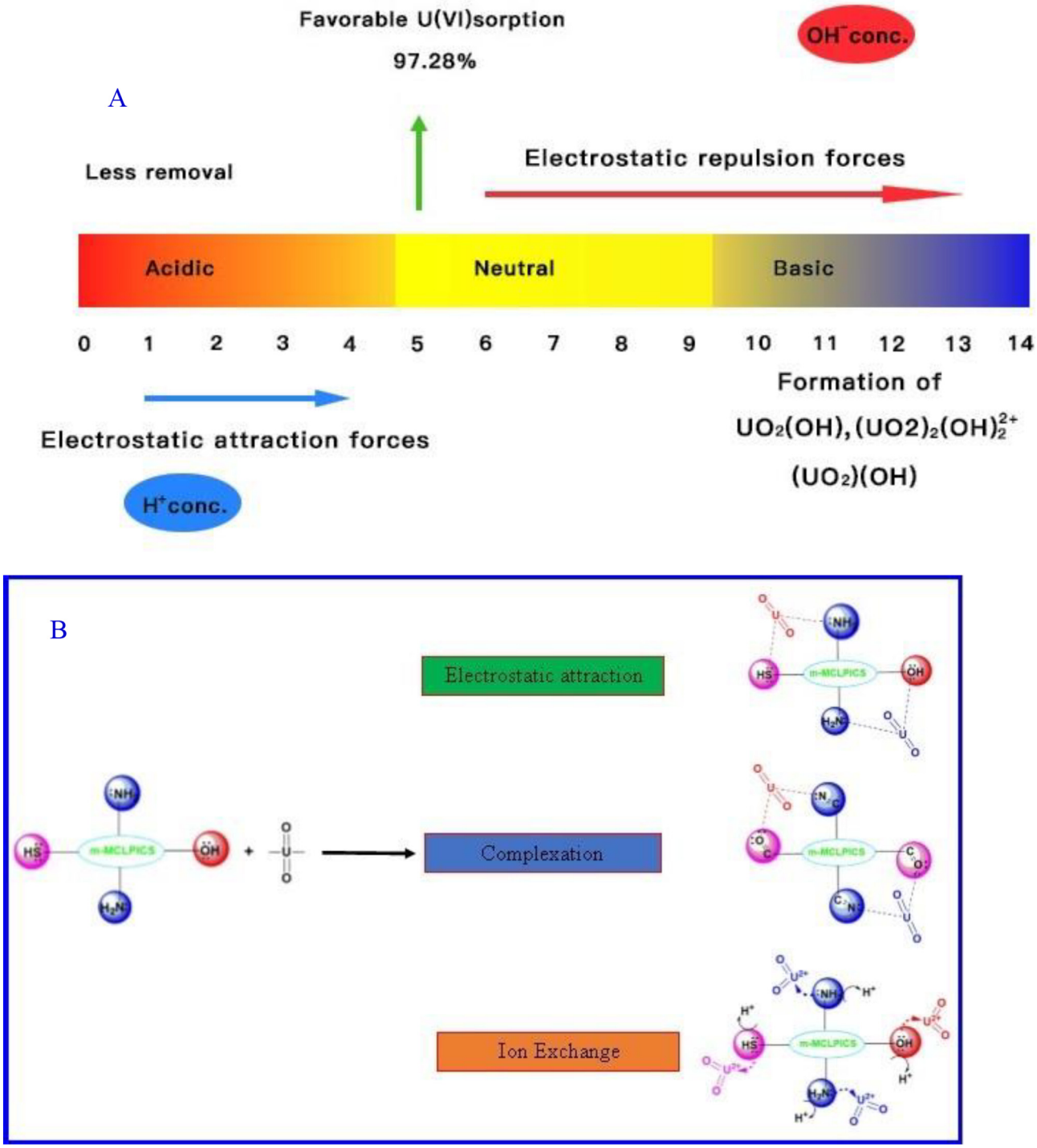

Fig. 6. (A) & (B) Mechanism of pH with U(VI) ions; (C) Effect of pH (Amount of Solution: 50 mL, U(VI) concentration: 40 mg/L, Contact time: 90 min, Temperature: 303 K); (D) adsorbent dose (Amount of Solution: 50 mL, U(VI) concentration: 40 mg/L, Contact time: 90 min, Temperature: 303 K, pH: 5.0); (E) contact time (Amount of Solution: 50 mL, U(VI) concentration: 20–80 mg/L, Temperature: 303 K, pH: 5.0, Amount of dose: 0.5 g); (F-I) kinetic evaluation plots (20, 40, 60 and 80 mg/L) (Amount of Solution: 50 mL, U(VI) concentration: 20–80 mg/L, Contact time: 90 min, Temperature: 303 K, pH 5.0, Amount of dose: 0.5 g); (J) Isothermal study (Amount of Solution: 50 mL, U(VI) concentration: 0–350 mg/L, Contact time: 90 min, Temperature: 303K, pH: 5.0, Amount of dose: 0.5 g); (K) temperature effect (Amount of Solution: 50 mL, U(VI) concentration: 20–80 mg/L, Contact time: 90 min, Temperature: 323 K, pH: 5.0, Amount of dose: 0.5 g); and (L) Thermodynamics of U(VI) onto m-MCLPICS, (M) Desorption of U(VI) ions with different eluents and (N) Adsorption-Desorption cycles of U (VI) onto m-MCLPICS.

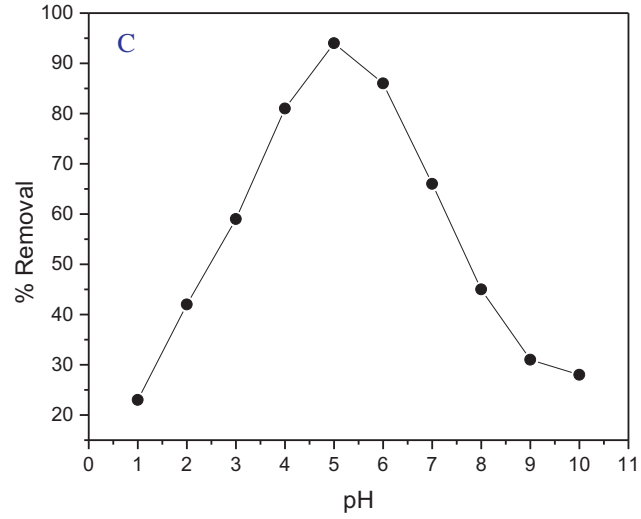

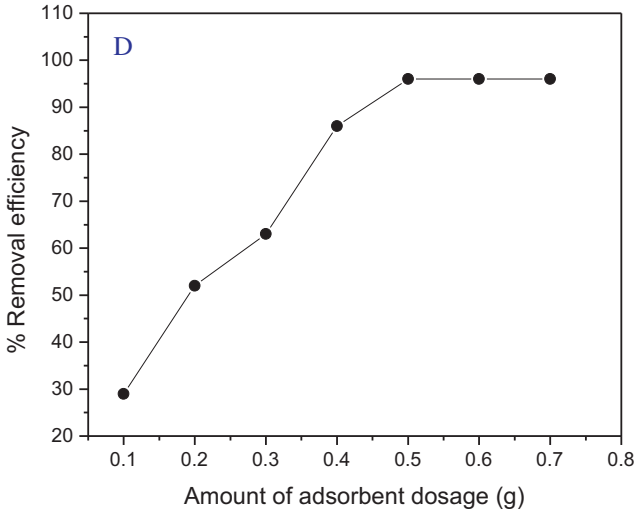

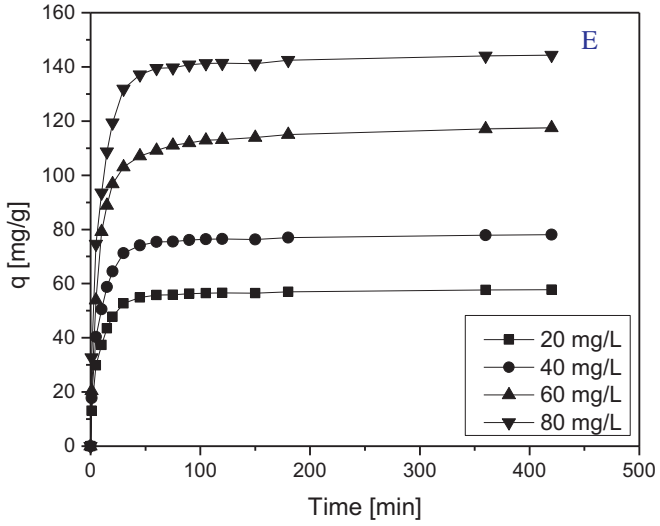

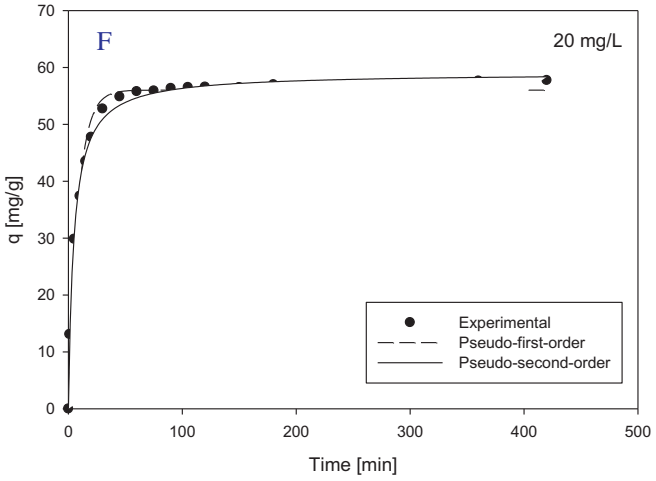

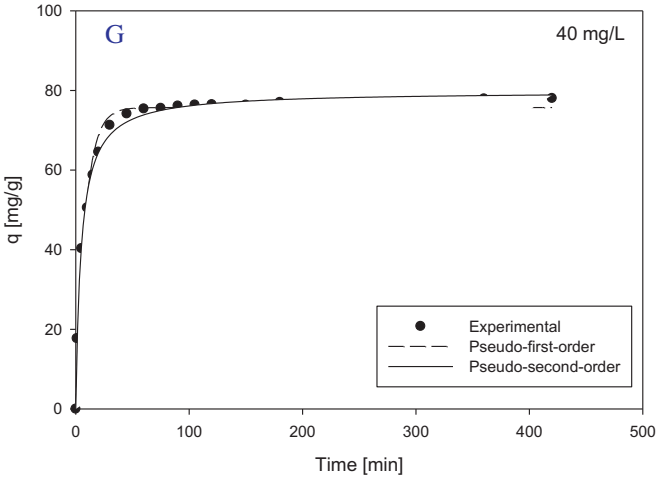

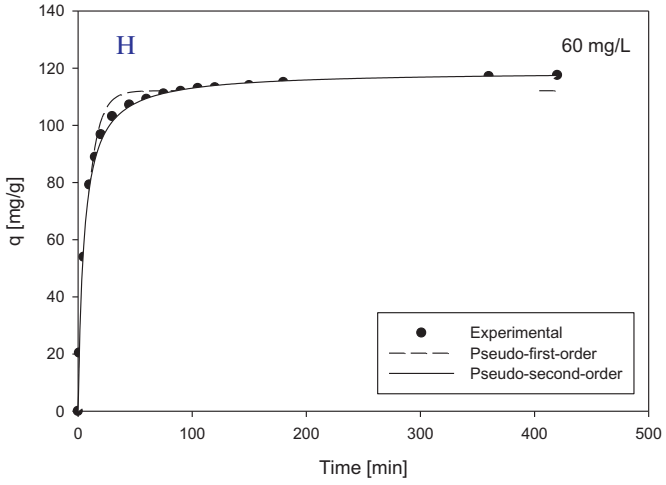

Fig. 6 (*continued*).

($R^2 = 0.999$) provided the best isothermal data for U(VI) adsorption with m-MCLPICS. The highest sorption capacity (q_m) and Langmuir constants of m-MCLPICS was calculated to be 250.7 mg/g at 323 K. The intention of this work is to improve the m-MCLPICS adsorption capacity. This implies that the functional groups of m-MCLPICS were uniformly occupied by the U(VI) and the monolayer or homogeneous adsorption

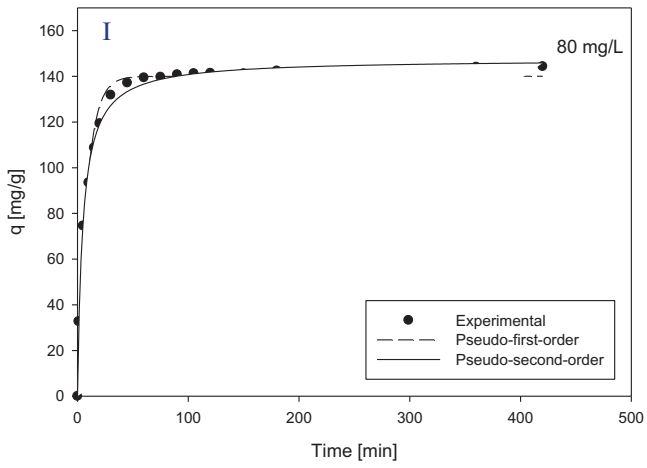

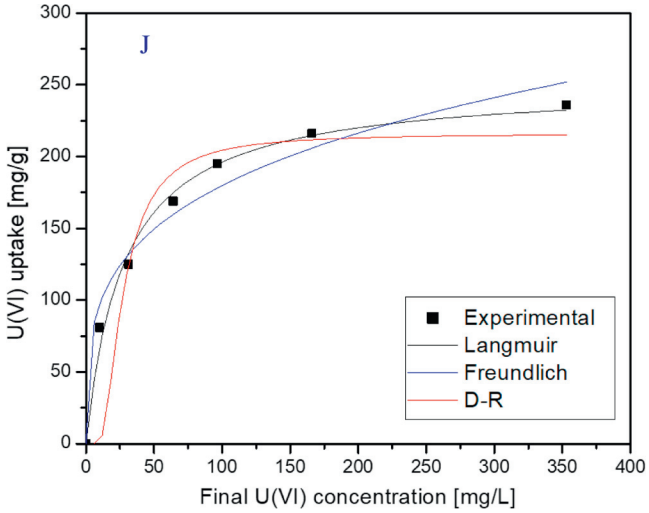

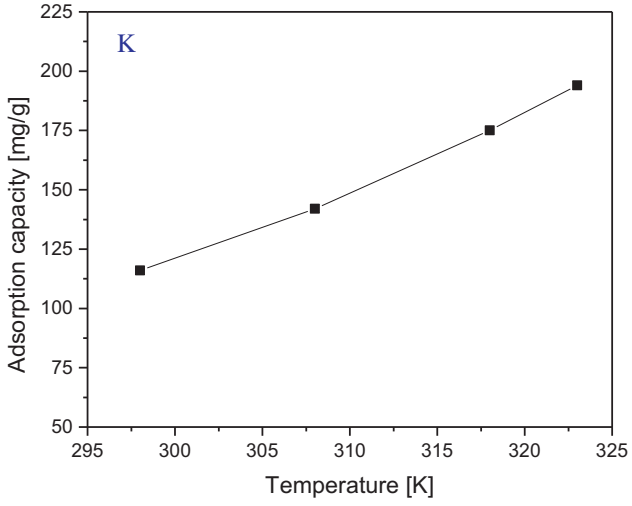

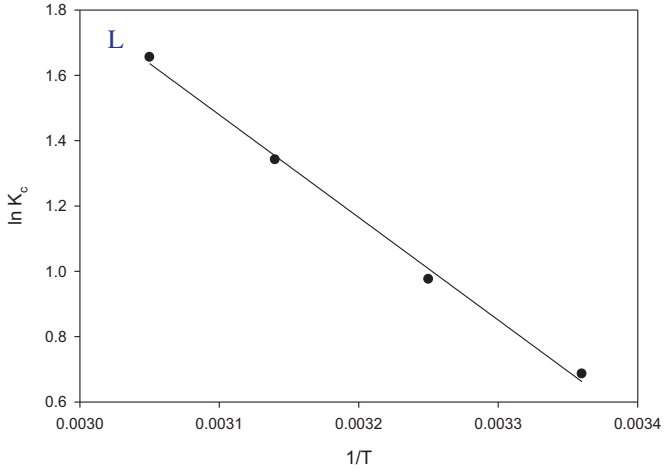

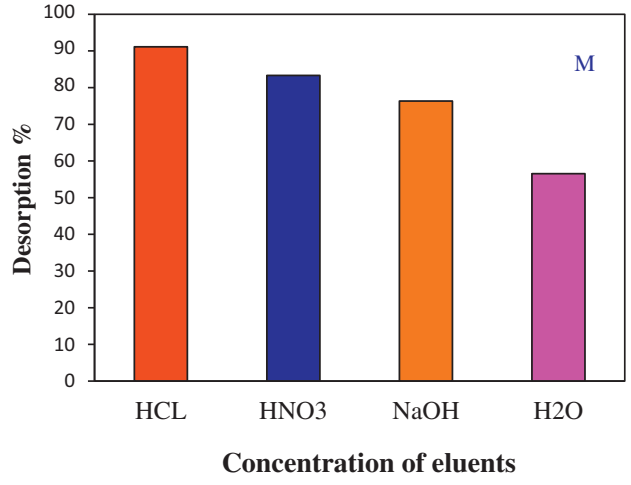

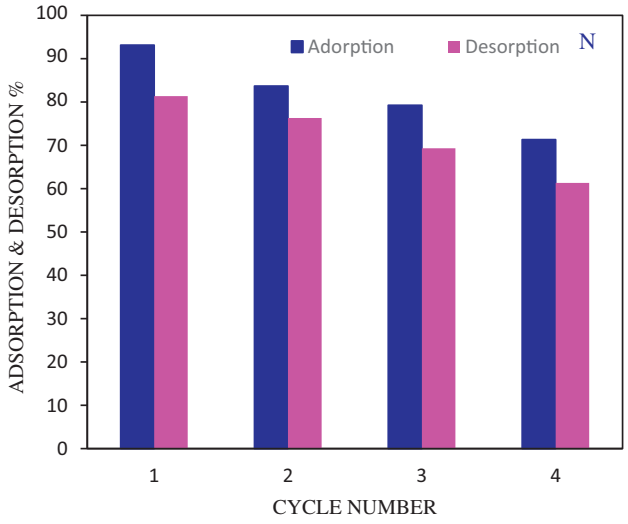

Fig. 6 (*continued*).

was the main mechanism in Langmuir isotherm. Freundlich model utilized to know the heterogeneous sorption system. R^2 and K_F values were compared with the Langmuir isotherm and the Freundlich isotherm has the lowest values than the Langmuir isotherm. This indicates that the Freundlich isotherm is not suitable for U(VI) sorption.

Affinity of the adsorbate towards adsorbent was studied with the help of dimensionless separation factor RL and it was represented by

Table 1
Kinetic parameter evaluation of U(VI) onto m-MCLPICS.

Adsorbent	U(VI) concentration	$q_{e,exp}$ (mg/g)	Pseudo-first-order model			Pseudo-second-order model		
			$q_{e,cal}$ (mg/g)	k_1 (L/min)	R^2	$q_{e,cal}$ (mg/g)	k_2 (g/mg·min)	R^2
m- MCLPICS	20	60.2	51.2	0.1183	0.9784	59.06	0.0035	0.9967
	40	79.1	68.7	0.1127	0.9714	79.8	0.0026	0.9949
	60	120.4	101.1	0.1134	0.9874	118.9	0.0016	0.9983
	80	151.4	140.1	0.1183	0.9795	149.5	0.0014	0.9956

the following equation.

$$R_L = \frac{1}{(1 + b\,C_0)} \tag{9}$$

R_L value indicates the adsorption process to be irreversible ($R_L = 0$), favorable ($0 < R_L < 1$), linear ($R_L = 1$) or unfavorable ($R_L > 1$). In this study m-MCLPICS having the 0.125 R_L value and it suggest that the U (VI) sorption was favorable.

In addition to the two isotherms D–R isotherm model was also applied to know the nature of sorption processes. The mean free energy of the U(VI) sorption can be determined by the following equation:

$$E = \frac{1}{\sqrt{2K}} \tag{10}$$

Free energy values describe the type of sorption mechanism. If E values existed 1–8 kJ/mol the sorption procedure can be considered as a physisorption processes and the E value lies between 8 and 16 kJ/mol, the sorption procedure is ion exchange. In this study the free energy values were calculated to be 2.012 to 3.012 kJ/mol, respectively. Hence the results indicates that the U(VI) removal in the present study is a physisorption process. The different isotherm parameters along with R^2 and χ^2 values are given in Table 2.

3.11. Effect of temperature with thermodynamic study

Toxic contaminants were released into the environment at various temperatures. Thus in the sorption process the temperature effect is an important parameter. Temperature strongly suggests whether the reaction is endothermic or exothermic during adsorption process. Temperature effects have been investigated under optimized conditions. U (VI) sorption is an endothermic because the sorption capacity increases as the temperature increases (Fig. 6K). The active sites have been activated with increasing temperatures and their number will increase. Moreover, they can generate sufficient energy to interact with surface sites. Increased temperature can also increases the U(VI) mobility. Thus, U(VI) can bind easily at higher temperatures with the m-MCLPIC. From Fig. 6K, it can be seen that the removal of U(VI) onto m-MCLPICS has the lowest sorption value at 298 K and the highest sorption value at 323 K, which means that highest temperature is favorable for U (VI) removal.

Thermodynamic parameters namely, Gibbs free energy (ΔG°), enthalpy (ΔH^0) and entropy (ΔS^0) values were obtained from the following equations:

$$K_c = \frac{C_{Ae}}{C_e} \tag{11}$$

$$\Delta G^\circ = -RT\ \ln K_c \tag{12}$$

$$\Delta G^\circ = \Delta H^\circ - T\Delta S^\circ \tag{13}$$

$$\ln K_c = -\frac{\Delta H^\circ}{RT} + \frac{\Delta S^\circ}{R} \tag{14}$$

where, C_{Ae} is the amount of U(VI) adsorbed on the solid phase at equilibrium, C_e is the equilibrium (final) concentration of U(VI), where, R is the universal gas constant (8.314×10^{-3} kJ/mol K), and T is the temperature (K). Thermodynamic parameters namely ΔG° and ΔH° can be utilized as a primary source to know the sorption procedure. ΔH^0 and ΔS^0 values were obtained from the plot of ln K_c versus 1/T (Fig. 6L). ΔG° suggests the feasibility of the system and the spontaneous existence of the adsorption at different temperatures. The negative values (−1.6999, −2.4994, −3.5476 and −4.5147 kJ/mol) of ΔG° showed that the adsorption of U(VI) onto m-MCLPICS was spontaneous system at the three experimental temperatures. Increased values ΔG° with temperature increases indicate the spontaneous adsorption of U(VI). The positive ΔH° value (25.1 kJ/mol) showed that the adsorption of U(VI) onto m-MCLPICS is an exothermic process. Whereas the positive ΔS^0 value (0.089 kJ/mol K) revealing that the enhanced randomness at the solid-solution system. Based on the above results thermodynamics of U(VI) onto m-MCLPICS was feasible, spontaneous and endothermic process.

3.12. Reusability

Desorption is a key mechanism from which the spent adsorbent is recovered and the targeted component will be eliminated. Desorption and reusability of m-MCLPICS onto U(VI) ions was explored in this regard and the findings were shown at Fig. 6M & N. A potential adsorbent must have a high adsorption capacity and a strong reuse property, which decreases wastewater treatment costs significantly. Throughout this study U(VI) desorption was examined with H_2O, NaOH, HCl and HNO_3 as a desorbing agents. The adsorbent was recycled multiple times in order to make the process inexpensive and feasible. With HCl, the maximum U(VI) desorption percentage was achieved. This can be because there is a repulsion in acidic pH between protonated amine groups with metallic ions that increases the process of desorption. From Fig. 6 M we can see that U(VI) ions were desorbed with the four consecutive desorption cycles with HCl solution as a desorbent agent. In contrast with the other desorbent agents, m-MCLPICS demonstrated a lower desorption using H_2O.

Table 2
Isotherm evaluation of U(VI) onto m-MCLPICS.

Isotherm	Parameters	Values
Langmuir	q_m (mg/g)	250.7
	K_L (L/mg)	0.036
	R^2	0.9923
	χ^2	34.5
Freundlich	K_f (mg/g)	52.6
	n	3.747
	R^2	0.9752
	χ^2	107.6
Dubinin-Radushkevich	Q_m (mg/g)	216.1
	K	0.0271
	R^2	0.5736
	χ^2	816.5

3.13. Effect of agitation speed

The U(VI) sorption onto m-MCLPICS was studied as a function of agitation time by varying in the range of 0–300 rpm and the obtained results were shown in Fig. 7A. The results show that, due to the presence of active vacant locations on the adsorbent surface, U(VI) increase as time increases. The removal rate of U(VI) is poor when the agitation rate is low. The inefficient dispersion of adsorbent into metal solution, leading to a decrease in U(VI) absorption, is possibly due to low speeds. U(VI) ions can be removed effectively by raising the agitation rate, leading to higher removal rates. It is possible to decrease the sorbent potential at a higher speed due to improper interaction between U(VI) ions and binding sites of the sorbent. Therefore, the agitation speed of 200 rpm was used for further studies.

3.14. Real Sample analysis

Experimental results shows that m-MCLPICS exhibited the highest sorption capacity to remove U(VI) from aqueous environment and the equilibrium reached within a short time. To evaluate the adsorption capacity of m-MCLPICS, the experiments were carried out for the removal of U(VI) from real polluted wastewater and the results were shown in Fig 7B & C. U(VI) contaminated wastewater was taken from uranium mines in South China. Before starting the experiments the polluted water concentration and pH were measured. Batch sorption experiments were performed with the polluted water. The concentration of uranium ions in it is 5.1, 1.79 and 0.54 g/L with the pH of 1.2, 3.3 and 8.1. It is well known that polluted water is a complex of different ions. The U(VI) removal percentage decreased in real polluted samples due to the competition of other ions with the active surface sites. Competition from other ions in will also leads to decrease U(VI) binding. For the three U(VI) concentrations the removal percentage of U(VI) increases with increasing the pH and dose. This is because the active sites have been increased with increasing the dose value. It is worth considering that m-MCLPICS has selectivity for U(VI), which might be worth further investigation in the field of advancement and separation of U from polluted water.

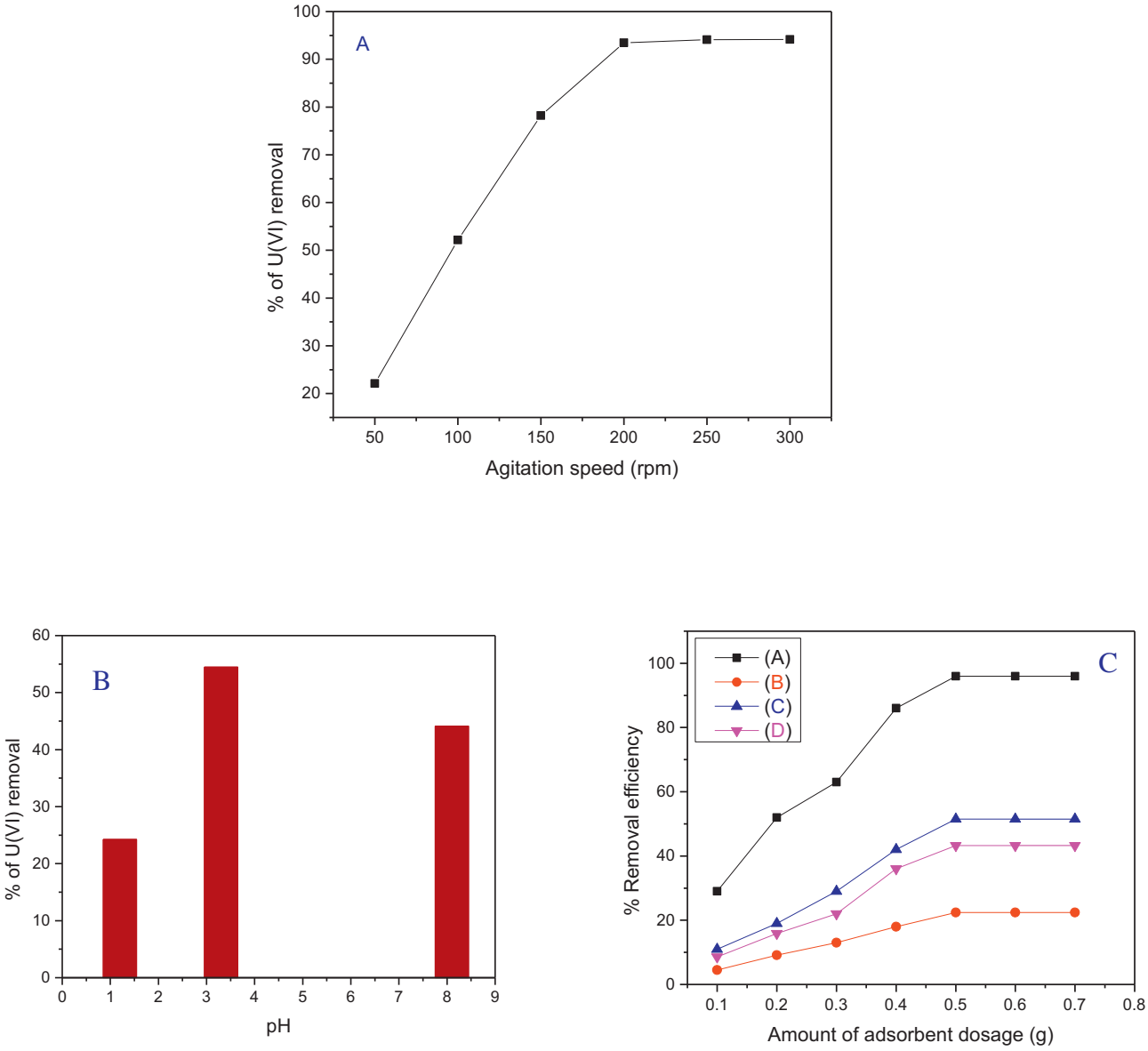

Fig. 7. (A) Effect of agitation speed; (B) Real sample pH (Amount of Solution: 50 mL, U(VI) concentration: 5.1, 1.79 and 0.54 mg/L, Contact time: 90 min, Temperature: 303 K, Amount of dose: 0.5 g); and (C) adsorbent dose (Amount of Solution: 50 mL, U(VI) concentration: 5.1, 1.79 and 0.54 mg/L, Contact time: 90 min, Temperature: 323 K, pH: 1.2, 3.3 and 8.1) on real polluted samples.

Table 3
Comparison of m-MCLPICS with other adsorbents.

Adsorbents	Experimental conditions	q_{max} (mg/g)	Reference
Amine modified silica gel	pH = 4.0, T = 302 K	35.86	[52]
SA@SiO_2	pH = 4.0, T = 298 K	44.5	[53]
Polymer supported primary amines	pH = 8.0, T = 296.15 K	14.80	[54]
TMP-g-AO	pH = 8.2 ± 0.1, T = 298.15 K	35.37	[55]
RGO	pH = 4.0, T = 293 K	47	[56]
Sulfonated GO	pH = 2.0, T = 293 K	45.05	[57]
GO/PPy	pH = 5.0, T = 298 K	147.06	[58]
Polyacrylamide-bentonite composite	pH = 5.0, T = 298 K	52. 1	[59]
m-MCLPICS	pH = 5.0 T = 303 K	250.7	Present study

3.15. Comparison study of m-MCLPICS

Sorption capacity of the adsorbent can be considered as a key point in practical point of view. m-MCLPICS sorption capacity was compared with other sorbents [52–59] and summarized in Table 3. m-MCLPICS has the maximum sorption capacity than the majority of other adsorbents reported in the literature. The superiority of sorption capacity for the current experiment was due to the introduction of lot of functional groups in the chitosan back bone structure. Modification of adsorbents may provide some specific extra functional groups and they can be contributed for the enhancement of U(VI) sorption. Thus it can conclude that m-MCLPICS has great tendency to remove U(VI) from aqueous as well as polluted samples.

4. Conclusions

In this work, m-MCLPICS was prepared, characterized and used under various conditions to remove U(VI) contaminants from the aqueous and polluted sea samples. BET, XRD, FTIR, SEM and VSM analysis was done to know the surface properties, crystalline, functional groups, surface morphology with elemental mapping, and magnetization of the adsorbent. The maximum (96%) removal percentage of U(VI) onto m-MCLPICS was obtained at pH 5. Adsorbent dose results indicate that the 0.5 g of sorbent dose is an optimal value for U(VI) removal. Pseudo-first-order, and pseudo- second-order, models were applied to explore the kinetic mechanism of m-MCLPICS towards U(VI) ions. Langmuir, Freundlich, and D-R models have been used to know the isotherm data. It was found that the kinetic data follows the pseudo-second-order model, and the equilibrium data fitted well with the Langmuir isotherm model. U(VI) removal of was favorable at higher temperatures and the maximum sorption capacity 250.7 mg/g was attained at 303 K. Therefore this study can also be regarded as novel, simple and inexpensive procedure for synthesizing the m-MCLPICS as an adsorbent through impregnation method with highest sorption performances of U(VI) from aqueous and sea samples.

CRediT authorship contribution statement

Gutha Yuvaraja: Writing - original draft, Writing - review & editing, Conceptualization. **Minhua Su:** Conceptualization. **Di-Yun Chen:** Supervision. **Yixiong Pang:** Conceptualization. **Ling-Jun Kong:** Supervision. **Munagapati Venkata Subbaiah:** Conceptualization. **Jet-Chau Wen:** Conceptualization. **Guda Mallikarjuna Reddy:** Conceptualization.

Acknowledgements

Corresponding author Di-Yun Chen is highly thankful to the National Natural Science Foundation of China (U1501231); The Project of Guangdong Provincial Key Laboratory of Radioactive Contamination Control and Resources (2017B030314182); Science and Technology Program of Guangzhou, China (201804020072) for providing the grant to carry out the research.

Reference

[1] Y.S. Wang, Y.T. Chen, C. Liu, F. Yu, J. Nucl. Mater. 504 (2018) 166–175.
[2] N. Hu, D.X. Ding, S.M. Li, X. Tan, G.Y. Li, Y.D. Wang, F. Xu, J. Environ. Radioact. 154 (2016) 60–67.
[3] Z. Zhang, H. Liu, W. Song, W. Ma, W. Hu, T. Chen, L. Liu, J. Environ. Radio. 192 (2018) 219–226.
[4] S. Yang, P. Zong, J. Hu, G. Sheng, Q. Wang, X. Wang, Chem. Eng. J. 214 (2013) 376–385.
[5] W. Liu, X. Dai, Z. Bai, Y. Wang, Z. Yang, L. Zhang, L. Xu, L. Chen, Y. Li, D. Gui, J. Diwu, J. Wang, R. Zhou, Z. Chai, S. Wang, Environ. Sci. Technol. 51 (2017) 3911–3921.
[6] M.O. Barnett, P.M. Jardine, S.C. Brooks, Environ. Sci. Technol. 36 (2002) 937–942.
[7] D.S. Alessi, B. Uster, H. Veeramani, E.I. Suvorova, J.S. Lezama-Pacheco, J.E. Stubbs, J.R. Bargar, R. Bernier-Latmani, Environ. Sci. Technol. 46 (2012) 6150–6157.
[8] C.S.K. Raju, M.S.A. Subramanian, J. Hazard. Mater. 145 (2007) 315–322.
[9] J. Li, Y. Zhang, Procedia Environ. Sci. 13 (2012) 1609–1615.
[10] A. Yao, T. Chu, J. Nucl. Phys. Mater. 480 (2016) 301–309.
[11] C. Zhou, A. Ontiveros-Valencia, L.C. de Saint Cyr, A.S. Zevin, S.E. Carey, R.K. Brown, B.E. Rittmann, Water Res 64 (2014) 255–264.
[12] S.W. Zhang, H.H. Gao, J.X. Li, Y.S. Huang, A. Alsaedi, T. Hayat, X.J. Xu, X.K. Wang, J. Hazard. Mater. 321 (2017) 92–102.
[13] R. Zhang, C.L. Chen, J. Li, X.K. Wang, J. Colloid Interface. Sci. 460 (2015) 237–246.
[14] A. Mittal, L. Kurup, V.K. Gupta, J. Hazard. Mater. 117 (2005) 171–178.
[15] V.K. Gupta, A. Mittal, L. Kurup, J. Mitta, J. Colloid Interface Sci. 304 (2006) 52–57.
[16] V.K. Gupta, A. Mittal, L. Krishnan, J. Mittal, J. Colloid Interface Sci. 93 (2006) 16–26.
[17] V.K. Gupta, R. Jain, S. Varshney, J. Hazard. Mater. 142 (2007) 443–448.
[18] V.K. Gupta, R. Jain, S. Varshney, J. Colloid Interface Sci. 312 (2007) 292–296.
[19] V.K. Gupta, I. Ali, V.K. Saini, Water Res 41 (2007) 3307–3316.
[20] V.K. Gupta, A. Rastogi, J. Colloid Interface Sci. 163 (2009) 396–402.
[21] V.K. Gupta, A. Mittal, A. Malviya, J. Mittal, J. Colloid Interface Sci. 335 (2009) 24–33.
[22] S. Karthikeyan, V.K. Gupta, R. Boopathy, A. Titus, G. Sekaran, J. Mol. Liq. 173 (2012) 153–163.
[23] V.K. Gupta, I. Ali, T.A. Saleh, A. Nayak, S. Agarwal, RSC Adv 2 (2012) 6380–6388.
[24] T.A. Saleh, V.K. Gupta, Environ. Sci. Pollut. Res. 19 (2012) 1224–1228.
[25] A.K. Jain, V.K. Gupta, S. Jain, Suhas, Environ. Sci. Technol. 38 (2004) 1195–1200.
[26] V.K. Gupta, S. Sharma, Ind. Eng. Chem. Res. 42 (2003) 6619–6624.
[27] V.K. Gupta, B. Gupta, A. Rastogi, S. Agarwal, A. Nayak, J. Hazard. Mater. 186 (2011) 891–901.
[28] A.K. Jain, V.K. Gupta, A. Bhatnagar, Suhas, Sep. Sci. Technol. 38 (2003) 463–481.
[29] A. Mittal, V.K. Gupta, A. Malviya, J. Mittal, J. Hazard. Mater. 151 (2008) 821–832.
[30] V.K. Gupta, R. Jain, A. Mittal, M. Mathur, S. Sikarwar, J. Colloid Interface Sci. 309 (2007) 464–469.
[31] A. Mittal, J. Mittal, A. Malviya, D. Kaur, V.K. Gupta, J. Colloid Interface Sci. 343 (2010) 463–473.
[32] V.K. Gupta, A. Rastogi, A. Nayak, J. Colloid Interface Sci. 342 (2010) 533–539.
[33] V.K. Gupta, A. Rastogi, J. Hazard. Mater. 52 (2008) 407.
[34] V.K. Gupta, I. Ali, Sep. Purif. Technol. 18 (2000) 131.
[35] G. Zhao, T. Wen, X. Yang, S. Yang, J. Liao, J. Hu, D. Shao, X. Wang, Dalton Trans 41 (2012) 6182–6188.
[36] A. Mellah, S. Chegrouche, M. Barkat, J. Colloid Interface Sci. 296 (2006) 434–441.
[37] Y. Liao, M. Wang, D. Chen, Ind. Eng. Chem. Res. 57 (2018) 8472–8483.
[38] A. Nilchi, S.T. Dehaghan, R.S. Garmarodi, Desalination 321 (2013) 67–71.
[39] G. Wang, X. Wang, X. Chai, J. Liu, N. Deng, Appl. Clay Sci. 47 (2010) 448–451.
[40] L. Zhou, C. Shang, Z. Liu, G. Huang, A.A. Adesina, J. Colloid Interface Sci. 366 (2012) 165–172.
[41] M. Sprynskyya, I. Kovalchuk, B. Buszewski, J. Hazard. Mater. 181 (2010) 700–707.
[42] M.K. Sureshkumar, D. Das, M.B. Mallia, P.C. Gupta, J. Hazard. Mater. 184 (2010) 65–72.
[43] L. Zhou, C. Shang, Z. Liu, G. Huang, A.A. Adesina, J. Colloid Interf. Sci. 366 (2012) 165–172.
[44] F. Noli, E. Kapashi, M. Kapnisti, J. Environ. Chem. Eng. 7 (2019) 102985.
[45] R.A.A. Muzzarelli, Carbohyd. Polym. 84 (2011) 54–63.
[46] S. Lagergren, K. Sven, Vetenskapsakad. Handl. 24 (1898) 1–39.
[47] Y.S. Ho, G. McKay, Process Biochem 34 (1999) 451–465.
[48] X. Zhang, C. Jiao, J. Wang, Q. Liu, R. Li, P. Yang, M. Zhang, Chem. Eng. J. 198 (2012) 412–419.
[49] I. Langmuir, J. Am. Chem. Soc. 40 (1918) 1361–1403.
[50] H.M.F. Freundlich, J. Phys. Chem. 57 (1906) 385–470.

[51] M.M. Dubinin, Chem. Rev. 60 (1960) 235–266.
[52] K.A. Venkatesan, V. Sukumaran, M.P. Antony, P.R.V. Rao, J. Radioanal. Nucl. Chem. 260 (2004) 443–450.
[53] F. Fan, D. Pan, H. Wu, T. Zhang, W. Wu, Ind. Eng. Chem. Res. 56 (2017) 2221–2228.
[54] R. Sellin, S.D. Alexandratos, Ind. Eng. Chem. Res. 52 (2013) 11792–11797.
[55] J. Zeng, H. Zhang, Y. Sui, N. Hu, D. Ding, F. Wang, J. Xue, Y. Wang, Ind. Chem. Res. 56 (2017) 5021–5032.
[56] Z.J. Li, F. Chen, L.Y. Yuan, Y.L. Liu, Y.L. Zhao, Z.F. Chai, W.Q. Shi, Chem. Eng. J. 210 (2012) 539–546.
[57] Y.B. Sun, X.X. Wang, Y.J. Ai, Z.M. Yu, W. Huang, C.L. Chen, T. Hayat, A. Alsaedi, X.K. Wang, Chem. Eng. J. 310 (2017) 292–299.
[58] R. Hu, D.D. Shao, X.K. Wang, Polym. Chem. 5 (2014) 6207–6215.
[59] U. Ulusoy, S. Simsek, O. Ceyhan, Adsorption 9 (2003) 165–175.